Research Square

Preprints are preliminary reports that have not undergone peer review.
They should not be considered conclusive, used to inform clinical practice,
or referenced by the media as validated information.

Environment-dependent diversity-stability relationship in microbial communities

Jiliang Hu

jilianghu@szbl.ac.cn

Shenzhen Bay Laboratory

Biological Sciences - Article

Keywords:

Posted Date: October 22nd, 2026

DOI: https://doi.org/10.21203/rs.3.rs-10960305/v1

License: This work is licensed under a Creative Commons Attribution 4.0 International License.
Read Full License

Additional Declarations: There is **NO** Competing Interest.

Abstract

Understanding the biodiversity–stability relationship has been a central challenge in ecology. Classical ecology proposed that diversity stabilize communities by distributing fluctuations across redundant pathways1,2, whereas random-interaction theory predicts that large and complex communities are unstable3,4. Field observations and experiments have reported positive, negative or negligible relationship between diversity and stability5–10. It therefore remains unclear diversity-stability relationship is universal or not and when a particular diversity–stability relationship emerges. Here we show that diversity-stability relationship is not fixed but environment-dependent, by studying bacterial communities under daily dilutions across temperature (10–50 °C) and dilution-rate (10^1–10^5) gradients. Communities exhibit two distinct fluctuation regimes: collective fluctuations and dominant-species fluctuations. In the collective fluctuation regime, many species interact and fluctuate together, and exhibit a positive diversity-instability relationship and turnover in the most abundant species. In the dominant-species fluctuation regime, only one or a few abundant species fluctuate and exhibit no significant diversity-instability relationship. Single species measurements show that the community fluctuation regime is determined by the balance between species growth and pH-mediated death. We developed a consumer-resource model with pH feedback reproducing both the fluctuation regimes and diversity–stability relationships observed in the experiment. We further tested our theoretical interpretation by performing another experiment tuning the dilution rate to shift between the same two regimes. Our results thus show that two distinct environment-dependent ecological mechanisms and fluctuation regimes lead to different diversity–stability relationships.

Introduction

How the biodiversity and stability of an ecological community arise from its species, and their shared environment is among the oldest questions in ecology. Its most enduring instance—whether greater diversity makes a community more or less stable—has divided ecologists for half a century. May's theoretical analysis predicted that species dynamics in random interaction networks become less stable as they grow more diverse and more strongly connected[3,4], whereas a long empirical tradition associated with Tilman and McCann found that diversity can stabilize aggregate ecosystem properties such as productivity[5,7]. Conflicting diversity-stability relationships have also been observed in different natural ecosystems and experiments[6,8–10]. Many such contradictions have been shown to stem from inconsistent notions of diversity and stability, such as different levels of aggregation[7,10–16]. Nevertheless, a central question remains: whether different diversity-stability relationships can reflect distinct dynamical regimes, where instability may be driven by different ecological mechanisms such as environmental variations or species interactions.

Microbial communities provide a tractable setting in which to address this question because diversity, environment and assembly can be manipulated directly while population dynamics are followed over many generations. In several synthetic microbial systems, instability increases with diversity or interaction strength, consistent with theoretical work showing that persistent fluctuations can be an

emergent collective effect of sufficiently complex interactions[17–23]. In such collective fluctuations, temporal variation occurs across many populations, and fluctuating communities are expected to be more diverse than stable communities within the same ensemble. This relationship, however, does not imply that every fluctuation in a diverse community has a collective origin, nor that diversity must predict instability under all environmental conditions.

Here we asked how environmental conditions shape the relationship between diversity and temporal instability in bacterial communities. Temperature is a key environmental variable which can reshape microbial communities by altering cellular growth physiology and metabolic acclimation[24,25], species interactions, and competitive outcomes[26–28], with consequences for community diversity and stability[29–31]. Mortality and dilution is another important environmental variable which can produce systematic shifts in microbial community composition by changing which growth strategies are favored[32]. Here, we studied microbial communities in different temperature conditions (10 to 50 °C). We found that varying temperature leads to both different ranges of diversity among surviving species, and different levels of correlation between diversity and instability, leading us to question the role of multi-species interactions in these relationships. Previous studies found that bacterial species notably interact by modifying and reacting to a shared abiotic variable such as pH[33,34]. We therefore characterized growth, pH modification and pH-induced within-cycle death of isolates to identify physiological features that could contribute to the observed fluctuating or stable dynamics. Species induce environmental deterioration (extreme pH) and therefore pronounced cell death (ecological suicide)[35] at higher temperatures (e.g. 40°C) than at optimal temperature (30°C). This strong within-cycle death rate can lead to single-species biomass fluctuations over serial dilutions. We next developed a daily-passage consumer–resource model and found that coupling resource use to a shared pH variable and pH-associated death was sufficient to generate stable, collective and dominant-species dynamics. Finally, we varied dilution factor at fixed temperature to determine whether the two fluctuation regimes also emerge along an environmental axis independent of temperature. The experiments establish environment-dependent fluctuation patterns; the model provides a possible dynamical interpretation rather than a direct identification of their experimental mechanism.

Temperature reshapes community dynamics and the diversity–instability relationship

We first tested how temperature alters the temporal dynamics of synthetic bacterial communities. Twelve communities, each assembled from a defined subset of a 25-isolate library, were inoculated at equal initial abundances into a complex medium containing glucose and urea (Fig. 1a; Materials and Methods). The isolate library spanned multiple phylogenetic groups (Fig. S1). Communities were propagated for ten daily passages by 1:30 dilution at 10, 20, 30, 40, or 50 °C, with three biological replicates per condition. Limiting the experiment to ten cycles was suggested in previous studies to ensure reproducible results by avoiding the onset of evolutionary dynamics, at the cost of short time series. At every passage, we added a community-specific dispersal inoculum at an effective rate of

approximately 10^{-6} to compensate for stochastic species extinctions. Daily measurements of optical density (OD), pH, and 16S rRNA amplicon composition allowed us to reconstruct biomass and species-resolved abundance trajectories.

The endpoint community biomass was similar at 20, 30, and 40 °C but substantially lower at 10 and 50 °C (Fig. 1b). Thus, communities at the three intermediate temperatures reached comparable biomass, even though their temporal dynamics differed markedly. The complete joint distributions of biomass and environmental pH over the temperature and dilution experiments are shown in Fig. S8.

We estimated the absolute abundance of each species as the community OD multiplied by its 16S relative abundance. Representative trajectories showed that the same inoculated community could be nearly stationary at one temperature but fluctuate strongly at another (Fig. 1c). Low temperature limited biomass accumulation, communities at 20 °C were comparatively stable, and multi-species fluctuations became prominent at 30 °C. At 40 °C, substantial temporal variation persisted despite reduced diversity, whereas at 50 °C only one or a few populations remained detectable and some trajectories approached collapse. The complete absolute- and relative-abundance trajectories across communities are shown in Figs. S2–S5. Temperature therefore changed the temporal dynamics of the constituent populations in addition to changing the total endpoint biomass.

We quantified population instability over passages 8–10 using two complementary metrics (Fig. 1d; Materials and Methods). Population instability (CV) was defined as $\Sigma_i \mathrm{SD}_t[N_i(t)]/\mathrm{Mean}_t[\Sigma_i N_i(t)]$, whereas population instability (std) was the corresponding non-normalized sum, $\Sigma_i \mathrm{SD}_t[N_i(t)]$. Both metrics quantify temporal variation across species and are distinct from variation in aggregate biomass. Absolute population variation was greatest at 30–40 °C. At 10 °C, low mean biomass elevated the normalized CV even though the non-normalized std remained small, indicating that these communities showed little absolute variation. Ranked instability distributions and sliding-window analyses supported the final-three-passage summary (Figs. S9 and S10).

Diversity followed a different temperature dependence. The endpoint Shannon diversity was highest at 30 °C and lower at the other temperatures (Fig. 1e), a pattern that was robust with alternative diversity metrics (Fig. S11). In particular, communities at 40 °C were less diverse than those at 30 °C despite having population instability of similar magnitude. Population instability therefore could not be inferred from diversity alone.

To compare diversity between communities with different levels of instability, we pooled all non-collapsed community–temperature observations, ranked them by population instability (CV), and divided them at the global median (Fig. 1f). At 20 and 30 °C, communities in the high-instability half were more diverse than those in the low-instability half ($P < 0.001$ for both comparisons), whereas no corresponding separation was evident at 10, 40, or 50 °C. Community 11 illustrates this contrast: the same two persistent species were comparatively stable at 20 and 30 °C but fluctuated strongly at 40 °C (Fig. S3).

Strong fluctuations can therefore occur in a low-diversity community even when greater diversity is associated with greater instability under other environmental conditions.

Temperature shifts the fluctuation regime and diversity-stability relationship through the growth–death balance

We next examined the diversity–instability relationship continuously within each temperature (Fig. 2a). Shannon diversity and population instability were positively correlated at 20 °C (Spearman $\rho = 0.53$, $P < 0.001$) and 30 °C ($\rho = 0.65$, $P < 0.001$), but not at 10 °C ($\rho = 0.07$, $P = 0.67$), 40 °C ($\rho = 0.19$, $P = 0.28$), or 50 °C ($\rho = 0.28$, $P = 0.46$). The positive associations at 20–30 °C were broadly consistent across alternative metrics, with metric-specific exceptions at other temperatures (Fig. S12), and an accumulated-diversity representation provided a complementary descriptive view of the temperature trajectories (Fig. S19). Thus, the diversity–instability relationship changed from no detectable association at 10 °C, to a positive relationship at 20–30 °C, and back to no detectable positive association among non-collapsed communities at 40–50 °C.

To identify physiological processes that could contribute to this regime shift of diversity–instability relationship, we characterized within-cycle dynamics of the 16 most abundant isolates in monoculture, recording OD, viable cell density, and culture pH over 24 hours (Fig. 2b). Representative isolates exhibited three outcomes. An acidifying isolate and an alkalinizing isolate both accumulated biomass and then lost several orders of magnitude of viable cells, whereas an isolate that returned toward a near-neutral pH retained high viability. In several trajectories, OD remained high after CFU (Colony-Forming Unit) count had declined, showing that the accumulated biomass did not necessarily represent the viable population available for the next passage. Additional temperature-resolved trajectories are shown in Fig. S13. These measurements link isolate-driven pH modification to within-cycle viability loss, although they do not distinguish pH stress from correlated physiological changes or accumulated metabolites.

We operationally classified a trajectory as showing clear within-cycle death when viable density declined by at least 1 $\log_{10}$ CFU ml^{-1} after reaching its within-cycle maximum (Fig. 2c; Materials and Methods). Across the 15 isolates with complete CFU measurements at 20, 30, and 40 °C, a substantial fraction met this criterion. The individual trajectories and their grouped means showed that death could follow either acidification or alkalinization, and the side distributions summarized both the magnitude of end-to-peak viability loss and the final pH of death and no-death trajectories. We therefore refer to this process as pH-associated death without attributing it to a particular direction of pH change or to pH alone.

Temperature altered both growth and end-of-cycle survival. End-of-cycle biomass measured by OD did not differ significantly among 20, 30, and 40 °C (Fig. 2d), but end-of-cycle viable density declined with increasing temperature and was lowest at 40 °C (Fig. 2e). Over the same range, exponential-phase growth rate increased progressively (Fig. 2f). Faster growth at 40 °C therefore produced comparable accumulated biomass but a smaller viable population at transfer, supporting greater within-cycle viability

loss rather than reduced biomass production. Additional analyses linked viability loss to both temperature and pH deviation (Fig. S14).

Controlling the initial pH independently revealed broad, species-specific physiological sensitivity (Fig. 2g). Integrated growth was generally greatest near the central pH range and was reduced at acidic or alkaline extremes, although the response differed substantially among isolates; the underlying growth trajectories are shown in Fig. S15. Species therefore differed both in how they modified environmental pH and in how their growth responded to the pH changes generated by themselves or by other community members.

Within-cycle viability loss provides a direct route from single-isolate physiology to inter-passage dynamics. A population can accumulate substantial biomass but contribute a much smaller effective inoculum if most cells lose viability before transfer. Repeated growth, viability loss, dilution, and dispersal can then amplify differences in viable carry-over. When many species grow and persist, their shared environmental feedback couples multiple populations and can generate joint fluctuations. When environmental filtering leaves only one or a few persistent species, the same feedback acts primarily within a dominant population, allowing boom–bust dynamics without a diverse interaction network. Collapse and subsequent regrowth at 50 °C represent an extreme realization of this growth–death–transfer sequence.

We summarized these observations in a conceptual growth–death landscape (Fig. 2h). As temperature increased from 10 to 40 °C, both growth and within-cycle death increased, shifting communities from a low-growth, low-absolute-variation regime at 10 °C, through collective fluctuations that were most prevalent near the growth optimum at 20–30 °C, to dominant-species fluctuations at 40 °C. At 50 °C, growth was strongly suppressed for many species and collapse became more frequent, consistent with an extension of the dominant-species regime into collapse–recovery dynamics. The temperature placements are ordinal rather than fitted, and collective and dominant-species fluctuations can coexist at the same temperature; environmental conditions change their relative prevalence rather than assigning every community to a unique state.

These results suggest that temperature shifts the prevalence of different fluctuation regimes. At temperatures favorable for the growth and persistence of many species, temporal variation is distributed across many coexisting species which interact with each other, producing collective fluctuations and a positive diversity–instability relationship. At high temperature, environmental filtering leaves fewer persistent species, and variation can instead be generated by one or a few dominant populations. Because these dominant-species fluctuations do not require a diverse interaction network, they need not be associated with increased community diversity. The thermal extremes were nevertheless distinct: communities at 10 °C had low absolute variation, whereas communities at 50 °C frequently contained only one or a few detectable species and sometimes underwent collapse followed by dispersal-assisted regrowth.

The isolate measurements identify environmental modification and within-cycle viability loss as prominent features of the culture system, but they do not determine the origin of any individual community trajectory. We therefore developed a consumer–resource model to test whether coupling resource use, a shared pH variable, and pH-associated death is sufficient to generate the three dynamical regimes and their contrasting diversity–instability relationships.

A pH-coupled consumer–resource model generates contrasting fluctuation regimes and diversity-stability relationships

The model describes species that compete for resources while jointly modifying a shared pH environment (Fig. 3a). Resource uptake produces species-specific growth and shifts pH according to resource-specific metabolic effects; deviation from each species' pH optimum produces pH-associated death. At the end of each 24-hour cycle, viable abundance is diluted and supplemented by dispersal, whereas resources and environmental pH are reset. This structure separates gross biomass production, which is compared with the experimental OD-based abundance, from the viable population transferred to the next passage.

The model generated stable, collective, and dominant-species dynamics (Fig. 3b). Stable communities converged to abundances that repeated across passages. Collective fluctuations involved persistent variation across many coexisting species when each species would be stable in isolation, whereas dominant-species fluctuations were concentrated in one or a few abundant populations. The within-cycle insets show how pH excursions and the resulting loss of viable cells can translate into passage-to-passage variation. These trajectories demonstrate behaviors that are possible within the model rather than assigning a unique mechanism to an experimental trajectory.

We simulated 5,000 independently assembled communities at each point in the parameter space defined by mean growth rate and death strength h (S = 12, M = 24, R_0 = 1). Outcomes were classified from the final three passages using the same population-instability metric as in the experiment. A bimodal distribution separated stable from fluctuating non-collapsed communities, whereas simulations with persistently low biomass were classified separately as collapsed (Fig. S16). The death-free control retained resource competition, pH modification, and pH-dependent uptake but removed pH-associated mortality.

The fraction of fluctuating communities was greatest where both mean growth and death strength were high (Fig. 3c). In the death-free limit, surviving communities converged to stable trajectories, showing that growth and environmental modification alone were insufficient under the simulated passage protocol. Conditional on pH-associated death, faster growth increased resource consumption and pH modification, thereby strengthening the feedback through which viability loss destabilized carry-over. Growth and death therefore acted jointly to promote inter-cycle instability.

The fluctuation-participation ratio showed that this unstable region contained two distinct organizations of temporal variation (Fig. 3d). At high growth and relatively moderate death, PR was comparatively high, indicating that variation was distributed across more species. This upper-left region of the parameter map corresponds to collective fluctuations: many species persisted, and modification of the shared environment by one population altered the growth and survival conditions of others. Consistent with this community-level origin, assembling otherwise stable model monocultures could generate persistent irregular fluctuations involving multiple species (Fig. S18). At high death relative to growth, PR declined toward the lower-right region, showing that variation became concentrated in fewer populations. Strong environmental feedback could then destabilize a dominant population through its own pH modification, producing single-species boom–bust or collapse dynamics.

These two fluctuation regimes produced different diversity–instability relationships (Fig. 3e). We quantified a diversity ordering as $\Delta P = \Pr(H_F > H_S) - \Pr(H_F < H_S)$, where H_F and H_S are the Shannon diversities of fluctuating and stable communities assembled at the same parameter values. ΔP was positive in the high-growth, moderate-death region: a fluctuating community was more likely to be more diverse than a stable community, consistent with collective instability emerging from a complex multispecies network. As death increased relative to growth, ΔP approached zero and became negative, indicating that fluctuating communities were no more diverse, and could be less diverse, than stable communities. Instability in this region was generated primarily by one or a few dominant populations and therefore did not produce a positive diversity–instability relationship. Fixed-growth slices through the parameter map showed the same progression (Fig. S17).

We integrated the fluctuating fraction, participation ratio, and diversity ordering into a schematic dynamical map (Fig. 3f). Low death favors stable dynamics; high growth with moderate death favors collective fluctuations; stronger death relative to growth favors dominant-species fluctuations; and low growth with strong death increases the chance of collapse. The experimental temperatures are located only qualitatively on this graph: 10 °C lies near the low-growth stable region, 20–30 °C near the collective-fluctuation region, 40 °C near the dominant-species region, and 50 °C near its collapse boundary. The boundaries summarize continuous ensemble trends rather than transitions, and the model does not map any experimental temperature to a unique parameter combination.

Dilution independently shifts the fluctuation regime and diversity-stability relationship

for environmental feedback to develop within each passage, rather than on temperature itself. We therefore propagated 12 communities assembled from an independent 36-isolate library for six daily cycles at 30 °C while varying the dilution factor from 10^1 to 10^5 (Fig. 4). Under weaker dilution, greater population carry-over allowed communities to reach high density earlier and spend more of each cycle in a late stationary-phase state. Stronger dilution reduced the initial abundance and delayed the return to high density, thereby shortening the time spent under late-cycle conditions. Species-resolved analyses used the one complete sequenced replicate available for each community–dilution combination, and the

full trajectories are shown in Figs. S6 and S7. Because dilution also changes bottleneck strength, demographic noise, and initial abundance, this experiment perturbs several processes affecting within-cycle feedback and cannot be interpreted as a direct manipulation of the model death parameter *h*.

Both normalized and non-normalized population instability decreased overall as the dilution factor increased (Fig. 4a). Thus, communities experiencing the weakest dilution—and therefore the greatest population carry-over—showed the largest inter-passage fluctuations. Although stronger dilution could in principle increase demographic noise or amplify discrete-time effects, the observed trend was in the opposite direction. This suggests that its dominant effect in our experiment was to attenuate the consequences of within-cycle environmental modification for viable carry-over. By delaying entry into stationary phase, stronger dilution likely reduced the time communities experienced extreme pH and associated viability loss before transfer, resulting in less pH-associated death, more consistent viable carry-over, and smaller fluctuations across passages. Endpoint Shannon diversity showed no corresponding monotonic trend across dilution factors (Fig. 4b). Passage conditions therefore altered population instability without producing a parallel change in endpoint diversity, further showing that diversity alone does not determine the magnitude of temporal variation.

We next related population instability to accumulated Shannon diversity, which summarizes the breadth and evenness of the populations contributing over the full analysis window (Fig. 4c). Rather than forming a single diversity–instability relationship, the observations revealed two characteristic regimes. In the upper, high-diversity branch, accumulated diversity showed a positive association with population instability, and the corresponding trajectories exhibited turnover among multiple fluctuating populations. In the lower, low-diversity branch, no clear diversity–instability relationship was evident, and fluctuations were repeatedly concentrated in one or a few dominant populations. These patterns correspond, respectively, to the collective-fluctuation and dominant-species fluctuation regimes identified in the temperature-gradient experiment. Marker shapes showed that collective fluctuations occurred across the dilution gradient, whereas dominant-species fluctuations were more frequent under weaker dilution. The heuristic thresholds at population instability (CV) = 0.25 and accumulated diversity = 0.8, together with the shaded regions, are descriptive guides linking observations to representative trajectories; they do not define fitted clusters or phase boundaries.

Changing the dilution factors at a fixed temperature therefore shifted both the magnitude and the organization of population fluctuations. Most importantly, the same two diversity–instability regimes observed across temperature re-emerged along this independent environmental axis: collective fluctuations were associated with a positive diversity–instability relationship, whereas dominant-species fluctuations showed no clear relationship.

Discussion

Our study reframes the diversity–stability question as one of fluctuation organization: environmental conditions change not only how strongly a community varies, but also whether that variation is

distributed across many populations or concentrated in one or a few dominant populations. These alternatives have different ecological origins. Collective fluctuations are emergent properties of multi-species coupling, whereas dominant-species fluctuations can be inherited from the dynamics of populations in isolation. The resulting diversity–instability relationship is therefore not an intrinsic property of the community; it is an emergent property of the coupled community–environment system. Collective and dominant-species regimes should be viewed as endpoints of a continuum whose relative prevalence shifts with the environmental context, rather than as mutually exclusive states.

In the collective regime, the same conditions that permit many species to coexist can also couple their dynamics through resource use and modification of a shared environment[36,37]. Realized diversity then expands the number of pathways through which changes in one population alter the growth or survival of others, providing a route from ecological complexity to endogenous temporal fluctuations[17,19–23]. This interpretation does not require diversity itself to causally increase instability. Instead, coexistence and broad participation in fluctuations can be joint consequences of the same environmental conditions and interaction structure. The mechanistically informative signature of collective fluctuations is not high diversity or large variance alone, but temporal variation distributed across many coexisting populations[38]. Additional hallmarks of collective fluctuations include turnover in the identity of dominant species and contrasts with the stability of individual populations grown in isolation. The experimental patterns are consistent with this interpretation, and the model shows that shared environmental feedback is sufficient to generate it; neither establishes the detailed interaction network operating in each experimental community.

The dominant-species regime reveals a distinct route to population-level instability. Environmental filtering can leave one or a few populations whose physiology and self-generated environmental feedback produce large changes in viable abundance. Rapid biomass accumulation followed by substantial within-cycle viability loss can, in principle, generate boom–bust dynamics across transfers without a diverse interaction network, as demonstrated by the model. Under these conditions, diversity is not required for fluctuation, and further filtering can reduce diversity while variation remains strong. Conversely, a weak diversity–instability relationship under slow-growth conditions can arise because little absolute variation develops. The same null correlation can therefore conceal two opposite dynamical situations—quiescent low-growth communities and strongly fluctuating low-diversity communities—showing why the correlation sign alone cannot identify the mechanism. Distinguishing them requires information about absolute variation, fluctuation participation, and the dynamics of candidate dominant species.

The growth–death–transfer balance provides a useful mechanistic coordinate system for understanding how environmental conditions shift the prevalence of these regimes. Growth renews biomass and accelerates resource consumption and environmental modification, whereas death translates environmental excursions into changes in viable carry-over. Transfer, in turn, determines how strongly these within-cycle effects propagate to the next cycle. In principle, more severe dilution could amplify fluctuations through two mechanisms: by increasing stochasticity in the smaller transferred populations

and by making population dynamics more discontinuous—and therefore more similar to discrete-time maps, which can readily exhibit cycles or even chaos. However, our experiment shows that increasing dilution suppresses fluctuations, suggesting that its dominant effect in our experiment is to attenuate the effect of within-cycle environmental modification on viable carry-over.

Our analysis concerns population-level instability, not variability of ecosystem function. In a collective regime, temporal asynchrony (turnover in which species dominates) allows large population fluctuations to coexist with relatively stable aggregate output[37,39,40]. In a dominant-species regime, functional consequences depend on whether ecosystem output is controlled by the fluctuating dominant taxon or buffered by other populations. A positive diversity–instability association at the population level therefore need not imply a similar impact on functional stability[7,10–16,41]. Connecting fluctuation regimes to functional stability requires joint measurements of species-level covariance and aggregate output.

The longstanding diversity–stability debate has persisted in part because studies conducted in different environments and at different observational scales have reported positive, negative, or absent relationships[3–16,29–31,41,42]. Our findings suggest that such contrasts need not reflect a single universal effect of diversity obscured by noise. Instead, within serially passaged microbial communities, environmental conditions altered the dynamical origin of temporal variation: when fluctuations were broadly distributed among coexisting populations, instability tended to be associated with higher diversity, whereas fluctuations carried by one or a few dominant populations decoupled diversity from instability and, in the model, could make fluctuating communities equally or less diverse than stable communities. The observed diversity–stability pattern was therefore contingent on which fluctuation regime prevailed rather than being a fixed property. Whether environment-dependent fluctuation regimes similarly determine diversity–stability relationships beyond microbial microcosms remains an open question. Future work should test this framework across spatial and temporal scales, levels of biological organization, trophic structures, and natural ecosystems, while jointly measuring population-level variation and aggregate ecosystem functions.

Declarations

Author contributions

Z.H. and J.H. conceived the study. Z.H. and J.T.L. performed the experiments. Z.H., J.H. and M.B. developed the theoretical model and analyzed the data. Z.H., J.H. and M.B. wrote the manuscript. J.H. and J.F.L. supervised the research.

Competing interests

The authors declare no competing interests.

Acknowledgements

We thank Lei Dai, Nieng Yan, Yaoqi Zhou and Terry Hwa for helpful discussions, and Amina Hadayat for preparing bacterial isolates.

References

1. Elton, C. S. *Animal Ecology* (Sidgwick & Jackson, London, 1927).
2. MacArthur, R. H. Fluctuations of animal populations and a measure of community stability. *Ecology* **36**, 533–536 (1955).
3. May, R. M. Will a large complex system be stable? *Nature* **238**, 413–414 (1972).
4. May, R. M. *Stability and Complexity in Model Ecosystems* (Princeton Univ. Press, Princeton, 1973).
5. Frank, D. A. & McNaughton, S. J. Stability increases with diversity in plant communities: empirical evidence from the 1988 Yellowstone drought. *Oikos* **62**, 360–362 (1991).
6. Rodríguez, M. A. & Gómez-Sal, A. Stability may decrease with diversity in grassland communities: empirical evidence from the 1986 Cantabrian Mountains (Spain) drought. *Oikos* **71**, 177–180 (1994).
7. Tilman, D., Reich, P. B. & Knops, J. M. H. Biodiversity and ecosystem stability in a decade-long grassland experiment. *Nature* **441**, 629–632 (2006).
8. Pfisterer, A. B. & Schmid, B. Diversity-dependent production can decrease the stability of ecosystem functioning. *Nature* **416**, 84–86 (2002).
9. Jiang, L. & Pu, Z. Different effects of species diversity on temporal stability in single-trophic and multitrophic communities. *Am. Nat.* **174**, 651–659 (2009).
10. Pennekamp, F. et al. Biodiversity increases and decreases ecosystem stability. *Nature* **563**, 109–112 (2018).
11. Tilman, D. Biodiversity: population versus ecosystem stability. *Ecology* **77**, 350–363 (1996).
12. McCann, K. S. The diversity–stability debate. *Nature* **405**, 228–233 (2000).
13. Loreau, M. & de Mazancourt, C. Biodiversity and ecosystem stability: a synthesis of underlying mechanisms. *Ecol. Lett.* **16**, 106–115 (2013).
14. Donohue, I. et al. Navigating the complexity of ecological stability. *Ecol. Lett.* **19**, 1172–1185 (2016).
15. Ives, A. R. & Carpenter, S. R. Stability and diversity of ecosystems. *Science* **317**, 58–62 (2007).
16. Isbell, F. et al. Predicting temporal stability and resilience from resistance and recovery. *Nature* **655**, 394–400 (2026).
17. Hu, J., Amor, D. R., Barbier, M., Bunin, G. & Gore, J. Emergent phases of ecological diversity and dynamics mapped in microcosms. *Science* **378**, 85–89 (2022).
18. Ratzke, C., Barrere, J. & Gore, J. Strength of species interactions determines biodiversity and stability in microbial communities. *Nat. Ecol. Evol.* **4**, 376–383 (2020).
19. Bunin, G. Ecological communities with Lotka–Volterra dynamics. *Phys. Rev. E* **95**, 042414 (2017).
20. Roy, F., Barbier, M., Biroli, G. & Bunin, G. Complex interactions can create persistent fluctuations in high-diversity ecosystems. *PLoS Comput. Biol.* **16**, e1007827 (2020).

21. Advani, M., Bunin, G. & Mehta, P. Statistical physics of community ecology: a cavity solution to MacArthur's consumer resource model. *J. Stat. Mech.* **2018**, 033406 (2018).
22. Marsland, R. III et al. Available energy fluxes drive a transition in the diversity, stability, and functional structure of microbial communities. *PLoS Comput. Biol.* **15**, e1006793 (2019).
23. Roy, F., Biroli, G., Bunin, G. & Cammarota, C. Numerical implementation of dynamical mean field theory for disordered systems: application to the Lotka–Volterra model of ecosystems. *J. Phys. A* **52**, 484001 (2019).
24. Knapp, B. D. & Huang, K. C. The effects of temperature on cellular physiology. *Annu. Rev. Biophys.* **51**, 499–526 (2022).
25. Knapp, B. D. et al. Metabolic rearrangement enables adaptation of microbial growth rate to temperature shifts. *Nat. Microbiol.* **10**, 185–201 (2025).
26. Burman, E. & Bengtsson-Palme, J. Microbial community interactions are sensitive to small changes in temperature. *Front. Microbiol.* **12**, 672910 (2021).
27. Lax, S., Abreu, C. I. & Gore, J. Higher temperatures generically favour slower-growing bacterial species in multispecies communities. *Nat. Ecol. Evol.* **4**, 560–567 (2020).
28. Abreu, C. I., Dal Bello, M., Bunse, C., Pinhassi, J. & Gore, J. Warmer temperatures favor slower-growing bacteria in natural marine communities. *Sci. Adv.* **9**, eade8352 (2023).
29. Zhao, Q. et al. Relationships of temperature and biodiversity with stability of natural aquatic food webs. *Nat. Commun.* **14**, 3507 (2023).
30. Ghosh, S., Matthews, B. & Petchey, O. L. Temperature and biodiversity influence community stability differently in birds and fishes. *Nat. Ecol. Evol.* **8**, 1835–1846 (2024).
31. García, F. C., Bestion, E., Warfield, R. & Yvon-Durocher, G. Changes in temperature alter the relationship between biodiversity and ecosystem functioning. *Proc. Natl Acad. Sci. USA* **115**, 10989–10994 (2018).
32. Abreu, C. I., Friedman, J., Andersen Woltz, V. L. & Gore, J. Mortality causes universal changes in microbial community composition. *Nat. Commun.* **10**, 2120 (2019).
33. Ratzke, C. & Gore, J. Modifying and reacting to the environmental pH can drive bacterial interactions. *PLoS Biol.* **16**, e2004248 (2018).
34. Ho, P. Y. et al. Resource competition predicts assembly of gut bacterial communities in vitro. *Nat. Microbiol.* **9**, 1036–1048 (2024).
35. Ratzke, C., Denk, J. & Gore, J. Ecological suicide in microbes. *Nat. Ecol. Evol.* **2**, 867–872 (2018).
36. Levine, J. M. & HilleRisLambers, J. The importance of niches for the maintenance of species diversity. *Nature* **461**, 254–257 (2009).
37. Loreau, M. & de Mazancourt, C. Species synchrony and its drivers: neutral and nonneutral community dynamics in fluctuating environments. *Am. Nat.* **172**, E48–E66 (2008).
38. Hu, J., Barbier, M., Bunin, G. & Gore, J. Collective dynamical regimes predict invasion success and impacts in microbial communities. *Nat. Ecol. Evol.* **9**, 406–416 (2025).

39. Zhao, L. et al. Biodiversity stabilizes plant communities through statistical-averaging effects rather than compensatory dynamics. *Nat. Commun.* **13**, 7804 (2022).
40. Wang, S. & Loreau, M. Ecosystem stability in space: α, β and γ variability. *Ecol. Lett.* **17**, 891–901 (2014).
41. Liang, M. et al. Unifying spatial scaling laws of biodiversity and ecosystem stability. *Science* **387**, eadl2373 (2025).
42. Mancuso, C. P., Lee, H., Abreu, C. I., Gore, J. & Khalil, A. S. Environmental fluctuations reshape an unexpected diversity-disturbance relationship in a microbial community. *eLife* **10**, e67175 (2021).

Figures

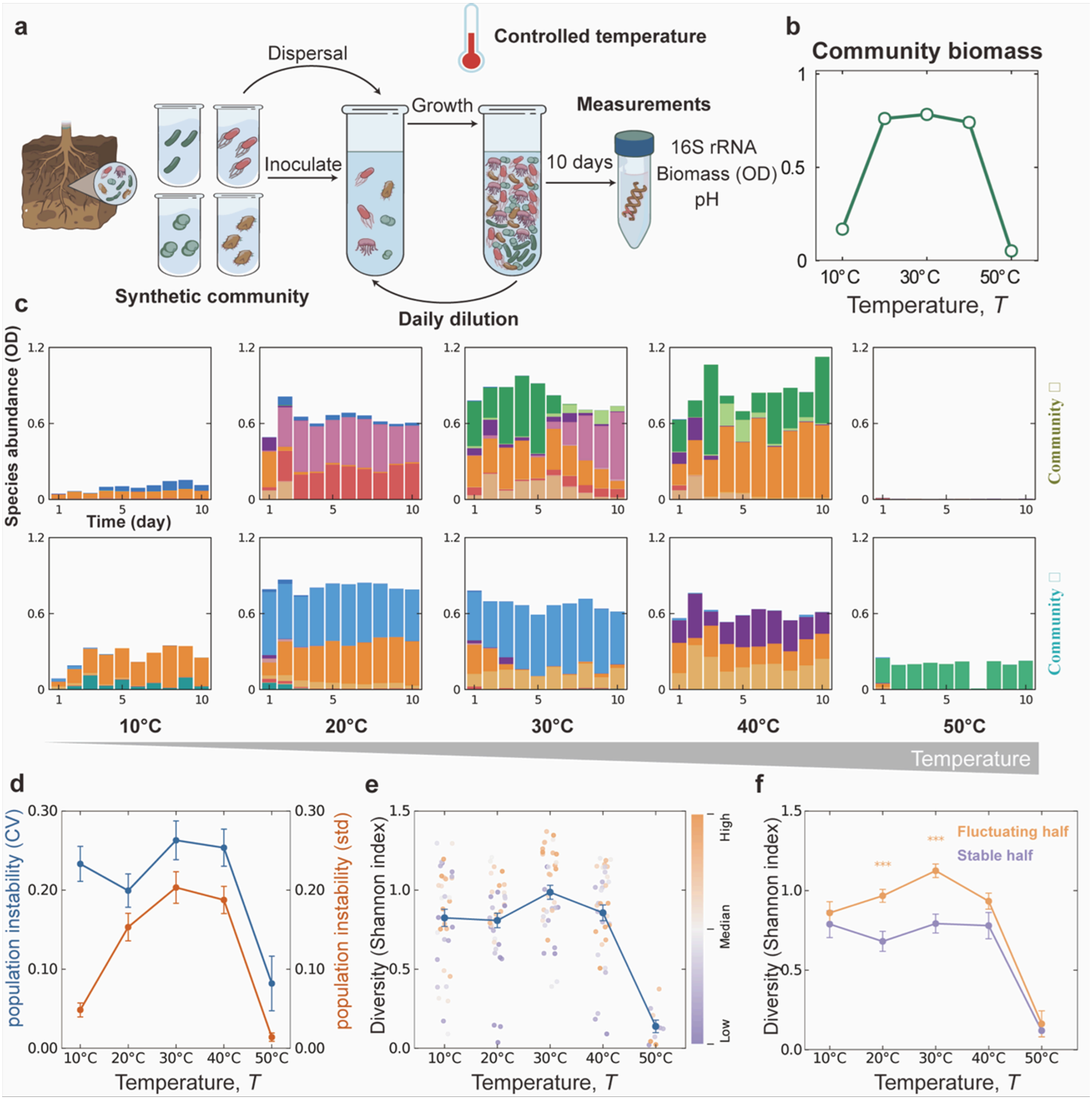


Figure 1

Temperature changes both population fluctuations and their relationship with community diversity. a, Experimental design: twelve synthetic communities assembled from a 25-isolate library were propagated by daily 1:30 serial dilution for 10 cycles at five temperatures (10–50 °C), with an approximately 10^{-6} community-specific dispersal pool added at each cycle; OD, pH and 16S rRNA amplicon composition were recorded daily. **b**, Endpoint biomass (OD) across temperatures. Biomass was similar at 20–40 °C and lower at 10 and 50 °C. **c**, Representative daily species-level abundance trajectories (OD × 16S relative

abundance) for two communities at each temperature. **d**, Population instability over the final three passages, quantified as $\Sigma_i SD_t[N_i(t)]/Mean_t[\Sigma_i N_i(t)]$ (CV, left) and $\Sigma_i SD_t[N_i(t)]$ (std, right; mean ± s.e.m.). e, Shannon diversity at each temperature; points are colored by population instability (CV) and the line shows the mean. f, Shannon diversity after ranking all community–temperature combinations by population instability (CV) and dividing them at the global median. Fluctuating communities were more diverse than stable communities at 20 and 30 °C but not at 40 °C (***P < 0.001, one-sided Wilcoxon rank-sum test).

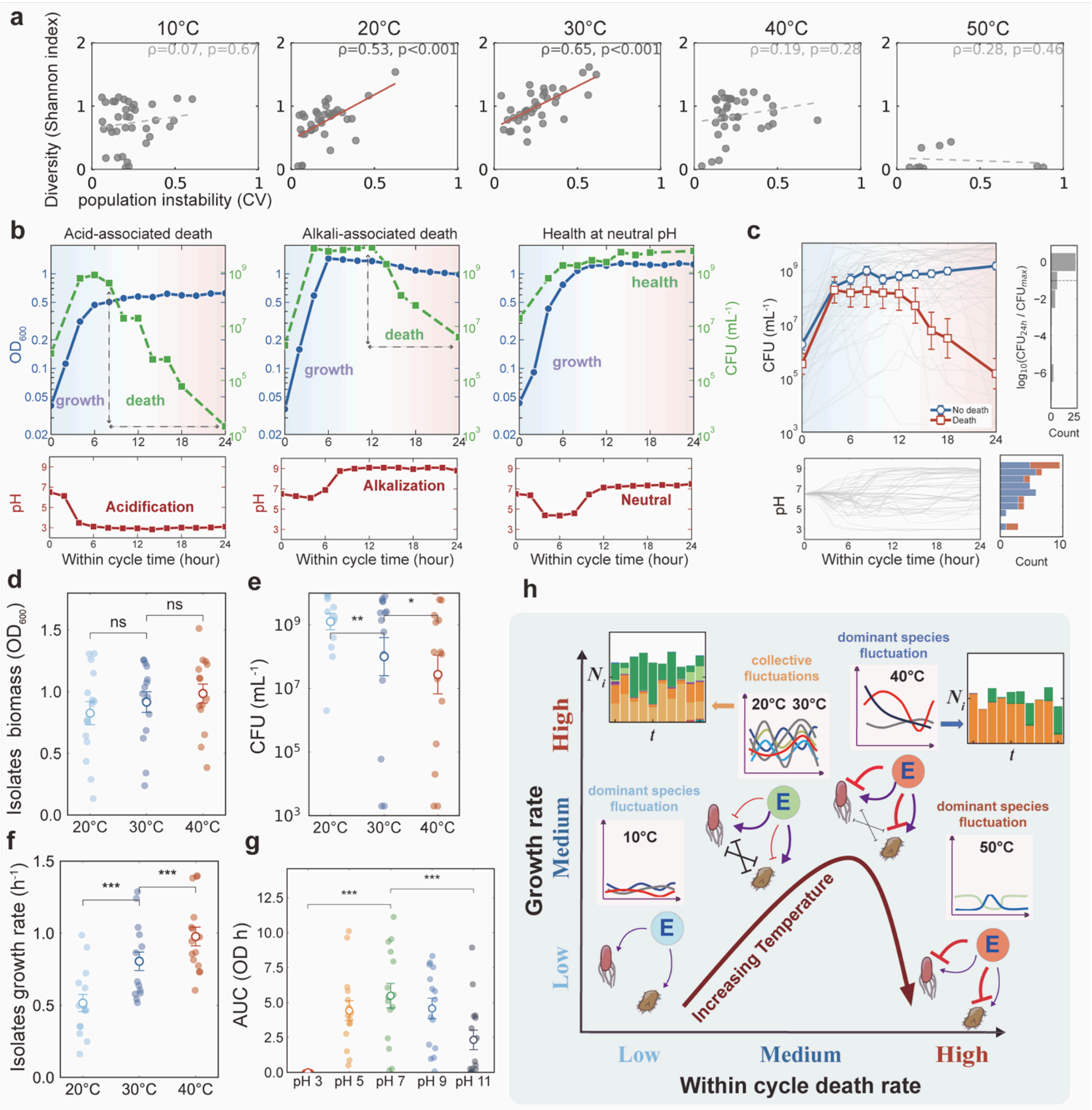


Figure 2

Temperature-dependent shifts in isolate growth and death coincide with changes in the diversity–instability relationship. a, Shannon diversity versus population instability (CV) at each temperature. Spearman *ρ* and *P* values are shown; the relationship was positive at 20 and 30 °C and not significant at 10, 40 or 50 °C. **b**, Representative within-cycle trajectories of monoculture OD_{600}, viable count and medium pH over 24 hours, illustrating pH modification associated with different degrees of viability loss. **c**, Viable-count trajectories for 45 isolate–temperature combinations from the 15 isolates with complete CFU measurements, classified as showing clear within-cycle death (≥1 $\log_{10}$ decline after the within-cycle maximum) or no clear death; side distributions show the end-to-peak CFU ratio and final pH. The threshold is operational and does not establish pH as the sole cause of death. **d**, End-of-cycle biomass (OD_{600}), which did not differ significantly among 20, 30 and 40 °C. **e**, End-of-cycle viable count (CFU ml^{-1}), which decreased with temperature. **f**, Exponential-phase growth rate, which increased with temperature (***$P < 0.001$). g, Integrated growth of 15 isolates across initial medium pH, showing heterogeneous pH sensitivity. **h**, Schematic organization of the experimental conditions by growth and within-cycle death. Temperature placements are ordinal, and collective and dominant-species fluctuations may coexist within a condition.

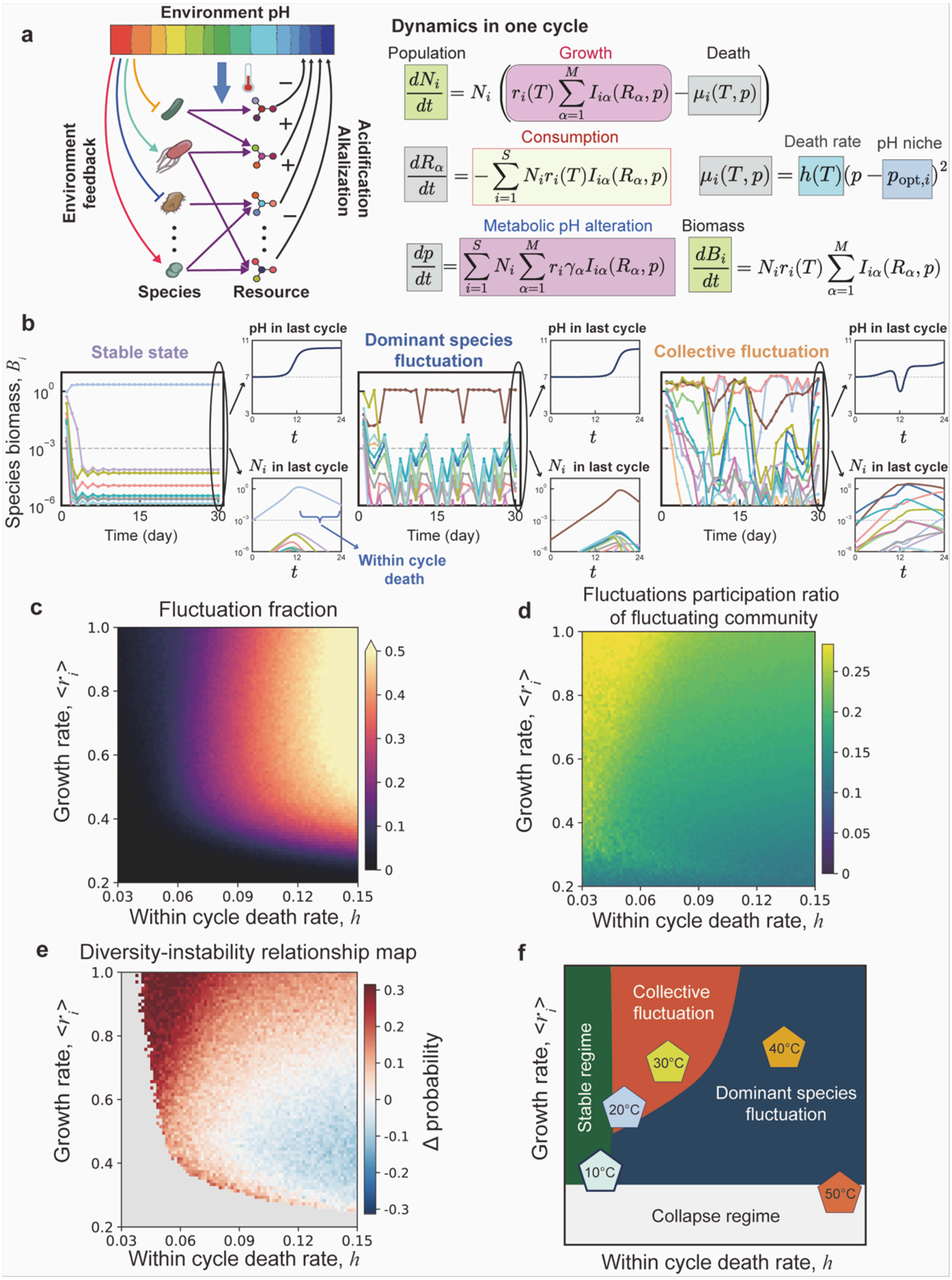


Figure 3

A pH-coupled consumer–resource model generates collective and dominant-species fluctuations with contrasting diversity–instability relationships. a, Daily-passage model in which species consume resources, modify a shared pH variable and experience species-specific pH-gated growth and pH-associated death (Eqs. 1–5). **b**, Representative stable, dominant-species and collective model trajectories. Main panels show passage-to-passage biomass, and insets show within-cycle pH and

population dynamics. **c–e**, Ensemble summaries across mean growth rate $\langle r_i \rangle$ and death strength h with $S = 12$, $M = 24$, $R_0 = 1$ and 5,000 random communities per parameter point. Metrics were calculated from the final three passages; $h = 0$ is the death-free reference and the main analysis spans $h = 0.03–0.15$. c, Fraction of communities classified as fluctuating from the bimodal distribution of population instability (CV). **d**, Normalized fluctuation-participation ratio, PR = $(\Sigma_i \sigma_i)^2/(S\Sigma_i \sigma_i^2)$, among fluctuating communities. e, Pairwise probability difference in Shannon diversity, $\Delta P = \Pr(H_F > H_S) - \Pr(H_F < H_S)$. f, Schematic dynamical summary of panels c–e. Boundaries are guides to continuous ensemble trends rather than fitted transitions, and experimental temperatures are placed ordinally rather than mapped to unique parameter values.

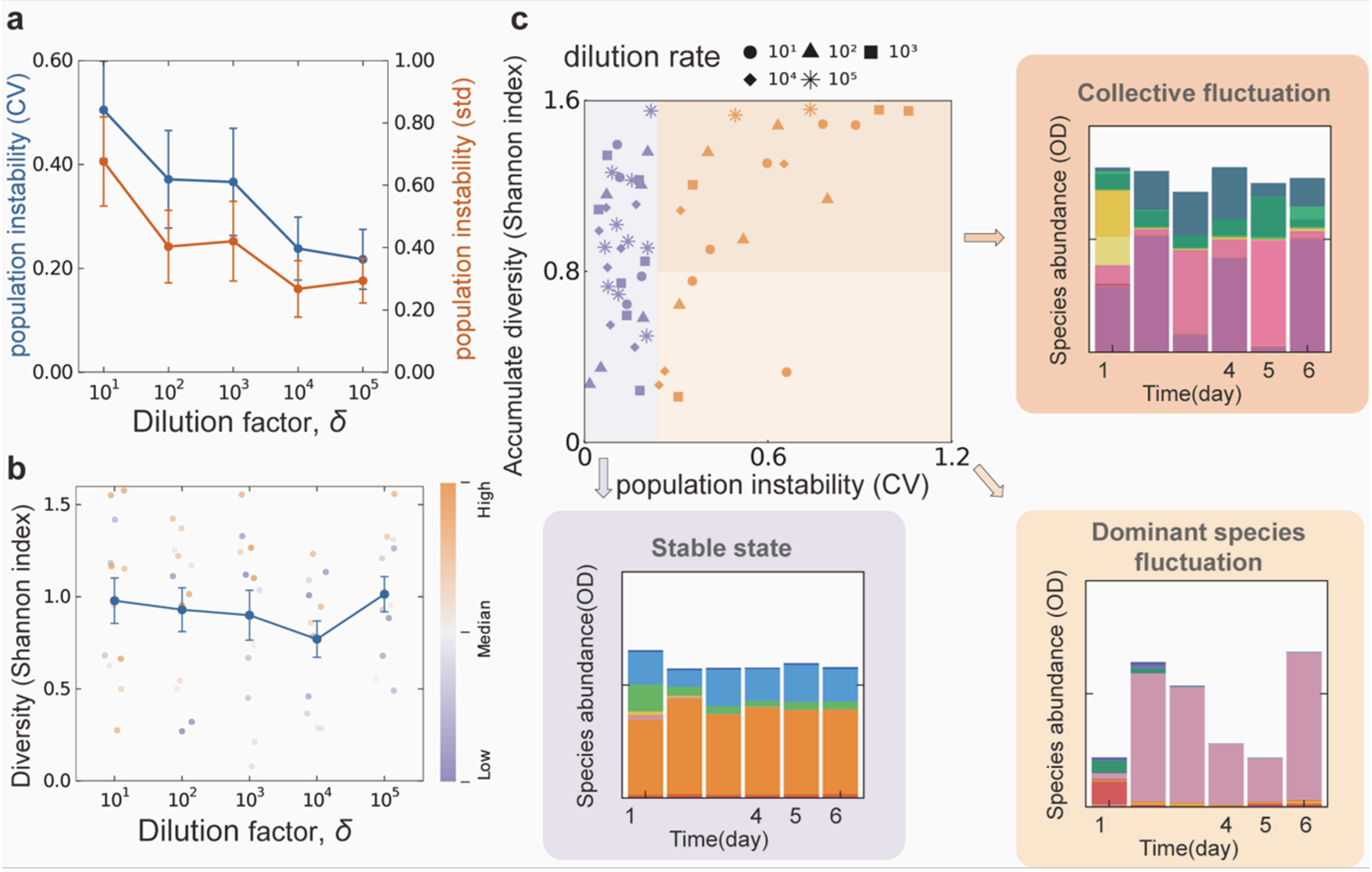


Figure 4

Changing dilution factor independently recapitulates the two fluctuation regimes and their contrasting diversity–instability relationships. Synthetic communities assembled from a 36-isolate library were propagated at 30 °C across daily dilution factors from 1:10^1 to 1:10^5. **a**, Population instability (CV and std) over the final three passages across dilution factors (mean ± s.e.m.). **b**, Shannon diversity across dilution factors; points are colored by population instability (CV) and the line shows the mean. **c**, Accumulated Shannon diversity versus population instability (CV) across all communities. Marker shape denotes dilution factor. Shaded regions are descriptive guides corresponding to stable communities,

collective fluctuations with high accumulated diversity and dominant-species fluctuations with low accumulated diversity. Insets show representative species-abundance trajectories.

Supplementary Files

This is a list of supplementary files associated with this preprint. Click to download.

- SupplementaryInformationNature.pdf